ELSEVIER

Journal of Hydrology 231–232 (2000) 233–243

Journal of Hydrology

www.elsevier.com/locate/jhydrol

Physics of water repellent soils

T.W.J. Bauters[a], T.S. Steenhuis[a,*], D.A. DiCarlo[b], J.L. Nieber[c], L.W. Dekker[d], C.J. Ritsema[d], J.-Y. Parlange[a], R. Haverkamp[e]

[a]*Department of Agricultural and Biological Engineering, Cornell University, Ithaca, NY 14853, USA*
[b]*Department of Petroleum Engineering, Stanford University, Stanford, CA 94035, USA*
[c]*Department of Biosystems and Agricultural Engineering, University of Minnesota, St. Paul, MN 55108, USA*
[d]*Alterra, Green World Research, P.O. Box 47, 6700 AA Wageningen, The Netherlands*
[e]*Laboratoire d'Etude des Transferts en Hydrologie et Environnement, BP 53-38041, Grenoble Cedex 9, France*

Received 2 April 1999; accepted 3 August 1999

Abstract

Although it is generally well known that water repellent soils have distinct preferential flow patterns, the physics of this phenomenon is not well understood. In this paper, we show that water repellency affects the soil water contact angle and this, in turn, has a distinct effect on the constitutive relationships during imbibing. Using these constitutive relationships, unstable flow theory developed for coarse grained soils can be used to predict the shape and water content distribution for water repellent soils. A practical result of this paper is that with a basic experimental setup, we can characterize the imbibing front behavior by measuring the water entry pressure and the imbibing soil characteristic curve from the same heat treated soil.

Keywords: Contact angle; Infiltration; Preferential flow; Fingered flow; Surfactant; Constitutive relationships

1. Introduction

Soils which have hydrophobic properties (also called water repellent soils) can resist or retard surface water infiltration (Brandt, 1969). Besides the retardation or resistance of surface water infiltration, water repellent soils have been associated with preferential flow (Jamison, 1945; Bond, 1964; Gilmour, 1968; Nissen et al., 1999). Preferential flow paths create spatial variability in soil moisture affecting plant growth (Dekker and Ritsema, 1994). In addition, preferential flow allows much faster transport of water and solutes, therefore creating a greater risk of groundwater contamination. It is important to predict water distribution and flow processes in water repellent soils and to understand how porous media theory developed for hydrophilic soils applies to hydrophobic soils. In a companion paper, the modeling of porous media flow in water repellent soils is reported (Nieber et al., 2000). This paper focuses on the physical interpretation of the infiltration experiments in hydrophilic and hydrophobic sands with the same textural composition, and on the effect of hydrophobicity on the water–energy relationships and resulting wetting front pattern.

The main difference between a hydrophilic and hydrophobic soil is the shape of the wetting front. Infiltrating water in a hydrophobic soil forms an

* Corresponding author. Tel.: +1-607-255-2489; fax: +1-607-255-4080.

E-mail address: tss1@cornell.edu (T.S. Steenhuis).

0022-1694/00/$ - see front matter
PII: S0022-1694(00)00197-9

Table 1
Infiltration experiment

Type of sand	Treatment	Infiltration fluid (surface tension, dynes/cm)	Drainage water (surface tension, dynes/cm)	Wetting potential (cm)	Front moisture content (cm^3/cm^3)	Porosity
Golf greens	Heat treated	70.01	69.91	−17.0	0.30	0.38
	Natural	71.37	60.72	3.0	0.34	0.38
	Natural (surfactant)	35.63	46.04	−3.5	0.31	0.38
Ouddorp 4–8 cm depth	Heat treated	65.10	62.41	−24.0	0.33	0.44
	Natural	65.10	51.28	NA	NA	NA
Ouddorp 20–30 cm depth	Heat treated	63.40	53.43	−17.0	0.31	0.41
	Natural	69.51	53.33	9.0	0.41	0.41
Ouddorp 60–70 cm depth	Heat treated	60.62	50.01	−19.0	0.32	0.40
	Natural	61.51	53.33	6.5	0.40	0.40

unstable front with fingers. In hydrophilic soils, water can infiltrate as a flat horizontal stable Richards' type-wetting front. According to Milly (1988), the wetting front in a hydrophobic soil is unconditionally stable when Richards' equation is used without hysteresis in the soil moisture characteristic curve (Nieber et al., 2000).

This paper is divided into several parts. In the first part, two sets of infiltration experiments using similar sands with different hydrophobicities are described and the results presented. In the discussion, the effect of water repellency on the constitutive relationships is discussed using the results of the experimental sets. Then, the wetting front behavior as a function of water repellency is discussed and, finally, a method for measuring water repellency is presented.

2. Materials and methods

2.1. Laboratory experiments

Two sets of infiltration experiments with water repellent sands were carried out in the Cornell High Energy Synchrotron Source (CHESS). The procedures and partial results of experimental set I were described earlier (Bauters et al., 1998) and are reanalyzed here. Experimental set II has recently been carried out and involves infiltration in chambers smaller than the diameter of the finger.

In experimental set I, hydrophilic sand was made hydrophobic by adding no (or 0), 3.1, 5, 5.7, and 9% by weight of extremely water repellent octadecyltrichlorosilane (OTS) sand. OTS sand was prepared by mixing sand with an ethanol solution containing 48 g/l OTS. Water repellencies of the mixtures were obtained that ranged from wettable to extremely water repellent. Infiltrations were carried out and imbibing and drainage curves of the constitutive relationships were measured in a polycarbonate chamber with interior dimensions of 45 cm wide, 57.5 cm tall, and 0.8 cm thick with 1 cm walls. The soil characteristic drainage curves were obtained by filling the chamber from the bottom with water. The water was turned off when the water level in the chamber reached the surface and the chamber was allowed to drain. After 24 h, the front panel of the chamber was removed and the sand at the right and left side of the chamber was segmented into 1 cm levels and moisture contents were determined by oven drying. The soil characteristic imbibition curves were also determined in the chamber; a constant head of 10 cm was connected to the bottom of the chamber and left connected for 24 h until equilibrium was reached. The chamber was again taken apart to section the sand and to determine the water saturation. In a separate experiment, the surface tension of the water was measured. More information is given in Bauters et al. (1998).

In experimental set II, water was infiltrated into a

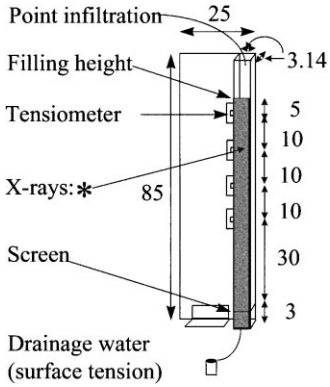

Fig. 1. Experimental set-up, all measurements are in cm.

3.1 cm square, 85 cm long polycarbonate chamber. Two naturally water repellent sands were used: Ouddorp sand in which Dekker and Ritsema (1994) and Ritsema et al. (1998) noted fingered flow, and water repellent golf greens sand used as the surface layer in golf greens (Kostka, 1997). Corresponding hydrophilic sands were made by "burning off" the organic matter by heating the soil to 600°C for 6 h. For all experiments, the sand was added to the chamber by pouring it continuously through a number of randomized screens. Distilled water (and in one case a surfactant solution consisting of 1% surfactant solution containing Primer 604® made by Aquatrols) was added at a rate of 10 cm^3 min^{-1} through a hypodermic needle located near the sand surface. Table 1 gives the details of the set of infiltration experiments. Matric potentials were measured with four fast responding miniature tensiometers (Selker et al., 1992a) positioned flush with the wall, 10 cm apart and starting 22 cm from the top (Fig. 1). Moisture content and soil density were measured with high intensity X-rays tuned to a fundamental energy of 40.7 keV provided by the A-2 beam line at the CHESS. Most of the details of this setup are discussed in DiCarlo et al. (1997) and Bauters et al. (2000). The only differences were that a Si(111) crystal was used instead of a Si(220) crystal for tuning the energy, and that the

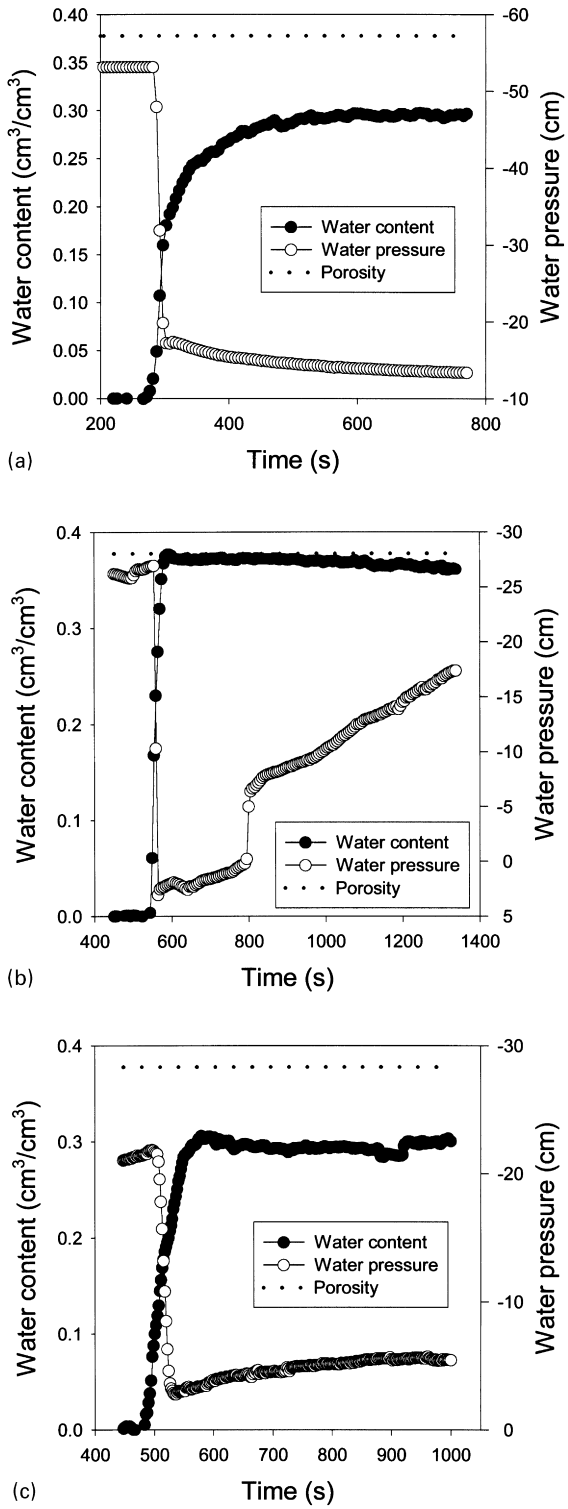

Fig. 2. Moisture content and matric potential at 15 cm depth for an infiltration experiment for a sand used in constructing golf course: (a) heat treated sand; (b) naturally water repellent sand; and (c) infiltration with Primer 604® (Aquatrols).

energies were recorded with xenon ion chambers which were more sensitive at high energies than the argon chambers employed by DiCarlo et al. (1997). The chamber was mounted on a movable x, y platform so that measurements could be taken at any position within the chamber. Both stationary and transect data were taken to document the moisture content. Stationary data were collected at the same height as the second tensiometer, 50 cm above the bottom of the chamber. The transect data were taken at a 1 cm interval from the bottom of the chamber till 65 cm height, positioned in the middle of the chamber. The drainage water was collected in 50 ml beakers and the surface tensions were measured with a Fisher Surface Tensiomat Model 21 where a platinum–iridium ring was suspended in the fluid to measure the apparent surface tension.

3. Results

Infiltration in the partly hydrophobic sand in experimental set I resulted in unstable fingered flow, while the hydrophilic sand (with the same textural composition) had the typical flat stable Richards' type wetting front. For the water repellent soil, the

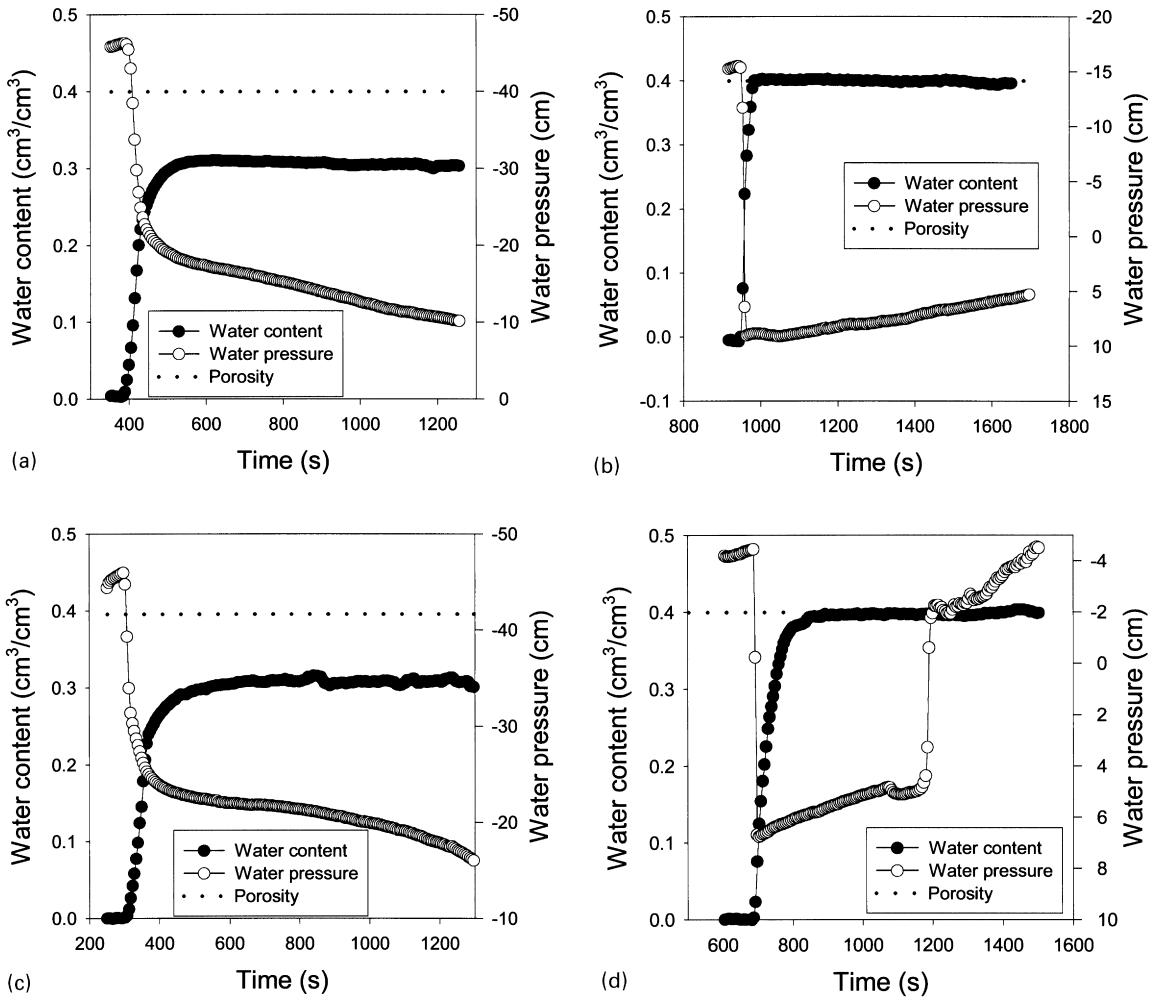

Fig. 3. Moisture content and matric potential for the Ouddorp sand: (a) 20–30 cm depth heat treated; (b) 20–30 cm depth naturally water repellent; (c) 60–70 cm depth heat treated; and (d) 60–70 cm depth naturally water repellent.

finger tip was saturated with a matric potential equal to the water entry value. Both moisture content and matric potential decreased behind the tip. The wetting front in the hydrophilic soil was unsaturated and the pressure increased slightly behind the front (Bauters et al., 1998). Those patterns were used in the validation of the finite element simulation by Nieber et al. (2000). Because of the artificial nature of our "constructed" sands, we used naturally repellent sands in the next set of experiments. We also used chambers that were smaller than the narrowest finger measured. Thus, for either a stable Richards' imbibing front or an unstable imbibing front, a flat imbibing front was obtained and, thereby, the compounding influence of the imbibing front shape on the moisture content and matric potential was avoided.

Experimental set II, with the 85 cm long and 3.1 cm square chamber, showed that the heat treated non water repellent golf greens sand had the typical stable Richards' type imbibing front behavior (Fig. 2a). The moisture content at the imbibing front was 0.30 cm^3/cm^3, which is less than the saturated moisture content (0.38 cm^3/cm^3). The matric potential at the imbibing front was −17 cm. Both matric potential and moisture content increased slightly behind the imbibing front and is characteristic for stable Richards' type imbibing fronts (Fig. 2a). The infiltration pattern for the "natural water repellent" golf greens sand was typical for unstable flow in water repellent sand despite that no finger formed and the water filled the whole chamber. Fig. 2b shows that the matric potentials were slightly positive at the imbibing front (3 cm) and then decreased behind the finger tip. The tip was saturated but the moisture content did not decrease behind the tip because, as is discussed later, the chamber was too short. When surfactants were added to the infiltrating water, the imbibing front had both hydrophobic and hydrophilic characteristics (Fig. 2c). The moisture content was 0.3 cm^3/cm^3 and the matric potential was −3.5 cm (Table 1).

For the Ouddorp sand, the same striking differences were observed between the water repellent and hydrophilic sands as for the golf greens sand with the exception for the severely water repellent sand taken from the 4–8 cm depth, where the water could not infiltrate even after 22 cm of water was ponded on top. This was surprising, as in the field the water infiltrated through this layer (Dekker, 1998). The water content and matric potential for the water repellent and heat treated soil for the 20–30 and 60–70 cm depths are shown in Fig. 3. The pattern is similar to the golf greens sand: In the partly hydrophobic soil, the moisture content was near saturation and the matric potential decreased behind the front (Fig. 3b and d); In the hydrophilic heat treated soil, the water infiltrated at moisture contents less than saturation and the matric potential slightly increased behind the imbibing front (Figs. 3a and c).

4. Discussion

The physical properties of water repellent soils (soil water characteristic curves and unsaturated conductivity) will be described first, followed by a discussion of how these properties relate to the wetting front patterns. The results from experimental sets I and II are used for illustrative purposes.

4.1. Soil water characteristic curves

The matric potential, ψ_m, in a pore with radius, r, is affected by the surface tension, σ, the contact angle, a, and the specific weight of water, ρ_w

$$\psi_m = -\frac{\sigma}{\rho_w g R} \tag{1}$$

$$R = \frac{r}{\cos a} \tag{2}$$

where R is the radius of the curvature of the water air meniscus, and g is the gravitational acceleration (Marshall et al., 1996).

Surface tension is influenced by heat treatment and surfactant solution. Table 1 shows that in the golf greens sand the surface tension of the drainage water for the hydrophilic heat treated soil is higher than that for the partly hydrophobic "natural soil". Interestingly, the surface tension of the drainage water for the natural soil, infiltrated with surfactant, increases. The surface tension of the drainage water for the Ouddorp sand is generally lower than the originally infiltrating water. Hydrophobicity also affects the matric potential through the contact angle (Eq. (2)). For contact angles less than 90°, water infiltrates under a negative pressure. Small pores fill up first, followed by successively larger pores. For

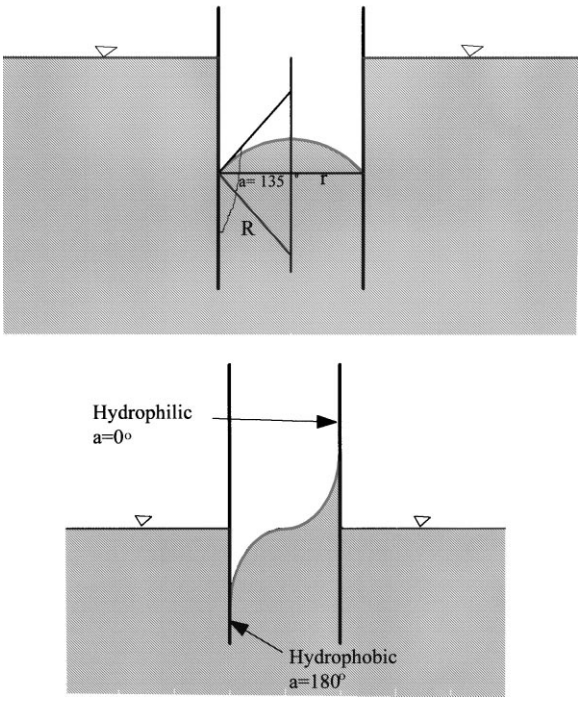

Fig. 4. Shape of meniscus between two plates: (a) uniform contact angle of 135°; and (b) one plate is hydrophobic ($a = 180°$) and the other hydrophilic ($a = 0°$).

contact angles greater than 90°, the matric potential of the infiltrating water in dry soils becomes positive. Now the big pores fill up first followed by the smaller pores. When the contact angle is 90°, all the pores will fill up simultaneously.

Fig. 4a shows a meniscus in a capillary tube with an uniform contact angle of 135°. In real soils, the surface is not uniformly covered with the hydrophobic material and there are individual small organic particles in the soil that contribute to the water repellency (Bisdom et al., 1993). To portray schematically the effect of pores with different contact angles, the meniscus between two plates, one hydrophilic ($a = 0°$), and the other hydrophobic ($a = 180°$), is drawn in Fig. 4b. The water–air surfaces will be much more complex in soils and we will use an effective contact angle that has the "same surface energy as the real meniscus". Obviously, the effective contact angle in Fig. 4b is 90°, indicating that two glass plates can be replaced by a medium of which the average contact angle is 90° and the meniscus is without curvature.

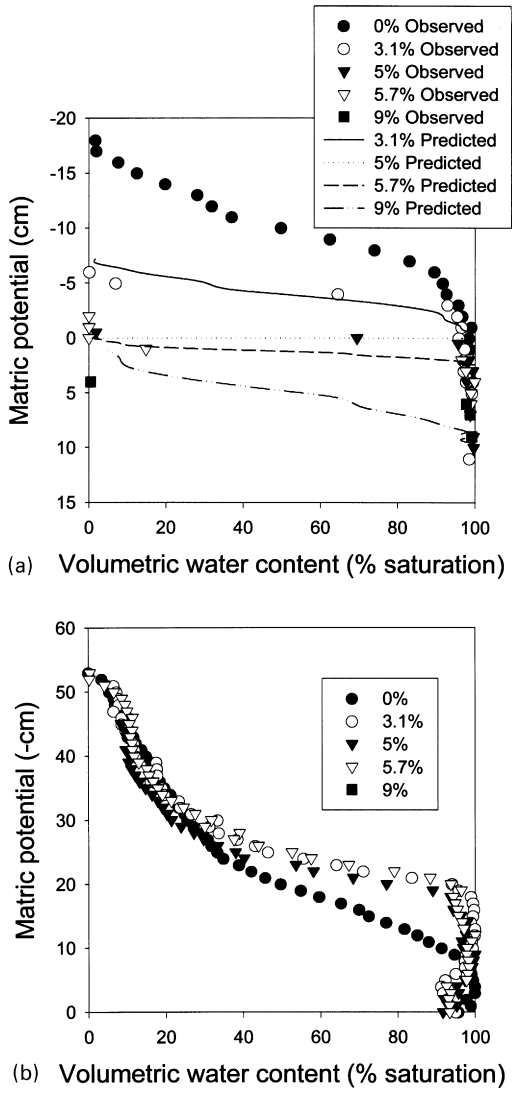

Fig. 5. (a) Predicted (lines) and observed (symbols) for the wetting curves of the same sands but with different degrees of water repellency (Bauters et al., 2000); and (b) drying curves.

Using the principle of effective contact angle, the wetting soil water characteristic curves from experimental set I are scaled (Miller and Miller, 1956) (Fig. 5). One difficulty is that the contact angles in soils cannot be measured independently. Therefore, one point of each imbibing curve is used to calculate the apparent contact angle and we then investigate how the other points on the curve scale with that contact angle. The best identifiable point is the water entry

Table 2
The water drop penetration time (WDPT) for the different batches[a]

Water repellency (%)	Water entry (cm)	Apparent contact angle (°)	WDPT (s)	Description
0	−7.5	0	<0.5	Wettable (<5 sec)
3.1	−3	67	40	Slightly water repellent
5	0	90	2400	Severely water repellent
5.7	1	98	>3600	Extremely water repellent
9.0	4	122	>3600	Extremely water repellent

[a] The WDPT test consists of randomly applying a single water drop (0.05 ml) onto the sand surface and measuring the amount of time (in seconds) it takes to infiltrate the soil (Letey, 1969; King, 1981).

value. This is the point where the largest pores fill up with water (Jury et al., 1991). For apparent contact angles smaller than 90° (i.e. where water infiltrates at negative pressures), the water entry value is identified by "the knee" in the imbibing soil characteristic curve near saturation. For water repellent soils ($a > 90°$) where the large pores fill up before the smaller pores, the corresponding water entry value is "the knee" near air dry. The apparent contact angles can be found as:

$$\cos a^{\mathrm{i}} = \frac{\sigma^{\mathrm{r}}}{\sigma^{\mathrm{i}}} \frac{\psi_{\mathrm{w}}^{\mathrm{i}}}{\psi_{\mathrm{w}}^{\mathrm{r}}} \cos a^{\mathrm{r}} \tag{3}$$

where the superscript r refers to the reference soil and the superscript i to the particular soil. The hydrophilic soil is used as the reference soil and assumes that the contact angle $a = 0°$.

This assumption is not a requirement but makes the discussion easier. The "water entry values" and the calculated apparent contact angles with Eq. (3) for the sand with different degrees of water repellencies are given in Table 2. The wetting curve for the 5% OTS sand is intriguing as it straddles the zero pressure line and an average contact angle of 90° was taken.

The imbibing curves for the partly hydrophobic soils can be derived from the hydrophilic soils by scaling with the contact angles from Table 2, as:
For $a < 90°$:

$$\psi^{i} = \frac{\sigma^{i}}{\sigma^{r}} \frac{\cos \mathrm{a}^{\mathrm{i}}}{\cos a^{r}} \psi^{r}, \qquad \theta^{\mathrm{i}} = \theta^{\mathrm{r}} \tag{4}$$

and for $a > 90°$:

$$\psi^{\mathrm{i}} = \frac{\sigma^{\mathrm{i}}}{\sigma^{\mathrm{r}}} \frac{\cos a^{\mathrm{i}}}{\cos a^{\mathrm{r}}} \psi^{\mathrm{r}}, \qquad \theta^{\mathrm{i}} = \theta_{\mathrm{s}} - \theta^{\mathrm{r}} \tag{5}$$

The calculated and observed imbibing curves are shown in Fig. 5a. The imbibing curves are generally well predicted except for the 9% OTS sand. A possible reason is that for the 9% OTS sand the capillary rise experiments might not be a good way to measure the imbibing loop of the soil characteristic curve, because of difficulty for water to enter the smallest pores.

Once water repellent soils are fully wet, the hydrophobicity disappears and, thus, the drainage curves should be the same. Fig. 5b shows that for experimental set I this is, in general, the case except for the 0% OTS sand which has a greater air entry value than the water repellent soils. A possible reason for the lower air entry value for the water repellent soils might be caused by the limited pressures during imbibing, which could result in a not fully imbibed medium, thus leaving the finer pores hydrophobic, which explains the lower air entry value.

The artificially prepared sands of experimental set I had only a small portion of the water repellent grains. In many regards, they are similar to naturally occurring sands where there is only a relatively small amount of hydrophobic material (Bisdom et al., 1993). The golf greens sand of experimental set II was prepared from taking hydrophilic sand and mixing it with less than 0.5% sterilized organic matter (Kostka, 1997). It is intriguing how such a small quantity of water repellent particles can affect the soil water behavior. To explain this, we note that in uniform sands each grain is surrounded by 10–12 grains (Hillel, 1980). Thus, for the 3.1% OTS sand, at most, 37% of the pore space between grains are affected by water repellent material. But, more significantly, more than half of the pore spaces are not affected by any water repellency and the water can move through these pore spaces easily, provided that they are connected. This was demonstrated by

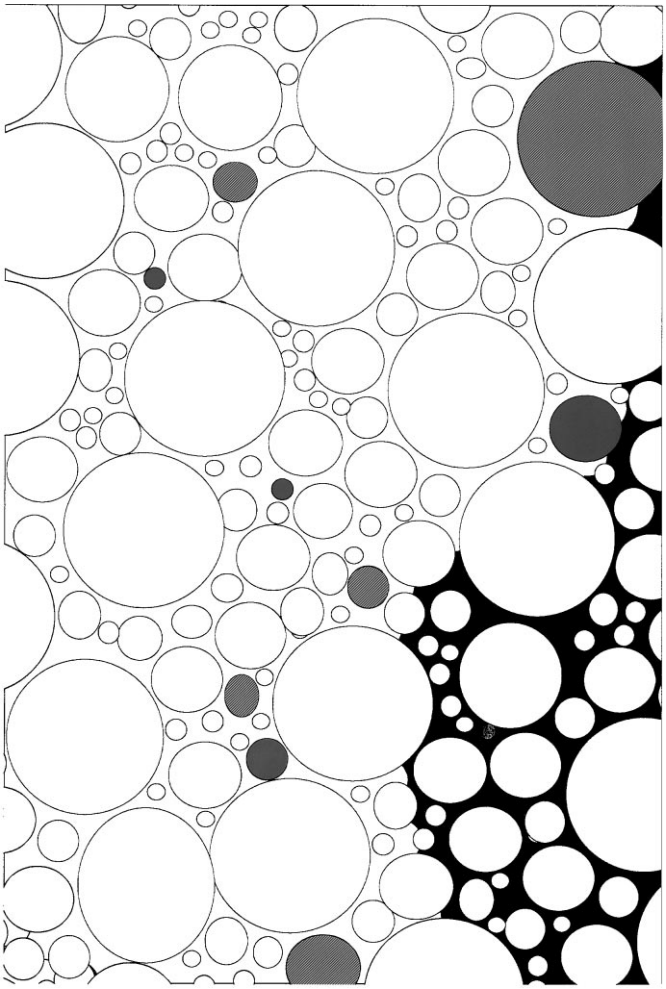

Fig. 6. Porous media with 3% of the grains (in solid) which are water repellent.

the water infiltration in the 3.1% OTS sand where the finger actually meanders, likely finding the least repellent soil. For the 5.7% OTS sand, up to 60% of the pore space is affected and for the 9% OTS sand, all the pore spaces would have at least one water repellent particle making the effective contact angle greater than 90°. Table 2 shows that, indeed, the water entry value is + 1 cm.

The sand in experimental set I was not uniform. In Fig. 6, a hypothetical heterogenous sand was constructed. Approximately 3% of the grains (colored in solid black) are water repellent. It is obvious that many passages are affected and only 20 to 30% of the pore spaces in the top section are still available for water to flow unhampered. If the water repellent particles are doubled to 6% (the additional grains are hatched) in some horizontal cross sections all pore spaces have one or two grains that are water repellent. In order for the infiltration front to pass these layers, the pressure needs to be positive. Once a pore is filled it can conduct water easily.

4.2. Unsaturated conductivity

It is generally assumed that the hydraulic conductivity is only a function of the moisture content (Jury et al., 1991; Hillel, 1980). As long as the contact angle is less than 90°, this is a reasonable assumption.

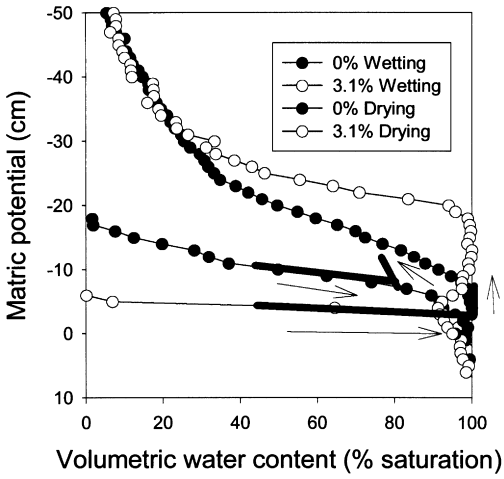

Fig. 7. Relationship between matric potential and moisture content when the matric potential is first increased, and then decreased by 2 cm. This hypothetical perturbation is depicted for a hydrophilic (0% OTS soil) and hydrophobic soil (3.1% OTS soil).

However, when the contact angle becomes greater than 90°, the large pores fill with water before the fine pores as for the more wettable soils. Thus, for soils with contact angles larger than 90°, we expect to see a higher conductivity at low moisture contents than for the wettable soils. DiCarlo et al. (1999b)showed the conductivity increased nearly linearly with moisture when the contact angle was affected by oil in the medium. Thus, for water repellent soils, there is hysteresis in the soil conductivity curve because different pores are filled for the same moisture content during imbibing and drying.

4.3. Stability of the imbibing front

The stability of the wetting front for different repellencies can be understood heuristically as follows. For density-driven displacements, the front is unstable whenever the flux, q, is less than the soil's unsaturated conductivity, $K(\theta)$ (Parlange and Hill, 1976):

$$q < K(\theta). \tag{6}$$

Results of experimental sets I and II show that, for water repellent soils, directly behind the wetting front the saturation is very high. This leads to a high conductivity and the instability criterion is satisfied for infiltration rates less than the saturated conductivity. Note that in hydrophilic soils the moisture content adjusts itself so that $q = K(\theta)$.

4.4. Moisture content and matric potential at the imbibing front

What is not obvious when unstable fingering occurs, is why the tip of the finger in dry soil is always saturated. The difference in moisture content and pressure between the unstable and stable Richards' imbibing fronts can only be explained when the pressure at the imbibing front varies slightly due to inhomogeneities or uneven distribution of water repellent particles. To illustrate this, let us assume that the moisture content at the imbibing front for the two different soils is the same as observed for the 0% OTS sand (i.e. 40% saturation). The matric potential for the 0% OTS sand is, then, −10.5 cm (D, Fig.7) and for the 3.1% OTS sand it is −4.5 cm (A, Fig. 7). When the matric potential hypothetically increases by 2 cm, the moisture content and matric potential relationship follows the main imbibing curve and the moisture content for the 0% OTS sand becomes 70% saturated (E, Fig. 7) and for the 3.1% OTS sand the moisture content becomes 100% saturated (B, Fig. 7). A smaller increase in matric potential will have the same effect but cannot be illustrated as well in Fig. 7. If the pressure is now decreased, a drying loop will be followed (Fig. 7). For the 3.1% sand, this means that the soil will remain saturated (C, Fig. 7) and for the 0% OTS sand, a secondary drying curve is followed and the moisture content will become approximately 65% saturated (F, Fig. 7). Repeated changes in pressure at the wetting front will follow the same secondary drying loop (Liu et al., 1995). Thus, we have shown that a small change in pressure together with hysteresis in the constitutive relationships, is responsible for the saturated moisture content of an unstable imbibing front.

4.5. Moisture content behind the finger tip

Selker et al. (1992b) noticed that the velocity, v, of the finger was constant. This was confirmed for water repellent soils by Bauters et al. (1998). Based on this constant velocity, v, the moisture content inside the finger can be expressed as $\theta(z - vt)$. Since the matric potential and $K(\theta)$ are only dependent on θ, we can define $\eta = z - vt$, and show that (Selker et al., 1996;

DiCarlo et al., 1999a):

$$\nu\theta_{\mathrm{w}} = K(\theta_{\mathrm{w}})\left(1 + \frac{\mathrm{d}\psi}{\mathrm{d}\eta}\right) \tag{7}$$

Eq. (7) can be integrated to give the moisture content and matric potential behind the finger tip. Of interest is to find the length of the saturated tip, L. At a particular time, Eq. (7) can be rewritten for the saturated finger tip and, after rearranging, gives the length, L, as:

$$L = \frac{\psi_{\mathrm{w}} - \psi_{\mathrm{a}}}{1 - \dfrac{\nu\theta_{\mathrm{f}}}{K_{\mathrm{f}}}} \tag{8}$$

where the subscripts w and a refer to water and air, respectively.

For water repellent soils, there is a large difference between the air entry value and the water entry value (Fig. 5a and b) compared to typical coarse grained soils, and we expect, therefore, long saturated tips as was observed for experimental sets I and II (Figs. 2 and 3).

4.6. Practical application

We have shown that the water entry value can be used to scale the wetting branches for a water repellent soil from the same soil that is heat treated. This suggests that a method to characterize the wetting front behavior may consist of measuring the water entry pressure and the imbibing soil characteristic curve of the same heat treated soil in which all the organic matter has been removed. These measurements are not difficult and require a segmented column, a Marriot bottle, a drying oven and a scale.

5. Conclusion

Two sets of experiments were carried out with similar sands that had different degrees of water repellency. Flat Richards' type of wetting fronts became unstable and formed fingers when the repellency increased. We found that soil physics theory developed for hydrophilic soils is valid for water repellent soils provided that the contact angle effect is included. Water repellency had a direct and predictable effect on the constitutive relationship during imbibing. This in turn affected the shape of the wetting front. A laboratory method is proposed for examining the instability of the front by measuring the air water entry value and the constitutive relationship of the particular soil after removing the organic matter.

References

Bauters, T.W.J., DiCarlo, D.A., Steenhuis, T.S., Parlange, J.-Y., 1998. Preferential flow in water repellent sands. Soil Sci. Soc. Am. J. 62, 1185–1190.

Bauters, T.W.J., DiCarlo, D.A., Steenhuis, T.S., Parlange, J.-Y., 2000. Soil water content dependent wetting front characteristics in sands. J. Hydrology, 231–232, 244–254.

Bisdom, E.B.A., Dekker, L.W., Schoute, J.F.Th., 1993. Water repellency of sieve fractions from sandy soils and relationships with organic material and soil structure. Geoderma 56, 105–118.

Bond, R.D., 1964. The influence of the microflora on the physical properties of soils II. Field studies on water repellent sands. Aust. J. Soil Res. 2, 123–131.

Brandt, G.H., 1969. Water movement in hydrophobic soils. Proc. Symp. Water Repellent Soils. Univ. Calif., Riverside, CA, pp. 91–115.

Dekker, L.W., 1998. Moisture variability resulting from water repellency in Dutch soils. Doctoral thesis, Wageningen Agricultural University, The Netherlands, 240pp.

Dekker, L.W., Ritsema, C.J., 1994. How water moves in a water repellent sandy soil. 1. Potential and actual repellency. Water Resour. Res. 30, 2507–2517.

DiCarlo, D.A., Bauters, T.W.J., Steenhuis, T.S., Parlange, J.-Y., Bierck, B.R., 1997. High-speed measurement of three-phase flow using synchrotron X-rays. Water Resour. Res. 33, 569–576.

DiCarlo, D.A., Bauters, T.W.J., Darnault, C.J.G., Steenhuis, T.S., Parlange, J.-Y., 1999a. Rapid determination of constitutive relations with fingered flow. In: Proc. International Workshop on Characterization and Measurement of the Hydraulic Properties of Unsaturated Porous Media. Riverside, CA. October 22–24, 1997, pp. 433–440.

DiCarlo, D.A., Bauters, T.W.J., Darnault, C.J.G., Steenhuis, T.S., Parlange, J.-Y., 1999b. Lateral expansion of preferential flow paths in sands. Water Resour. Res. 35, 427–434.

Gilmour, D.A., 1968. Water repellence of soils related to surface dryness. Aust. For. 32, 143–148.

Hillel, D., 1980. Fundamental of Soil Physics, Academic Press, New York (413pp).

Jamison, V.C., 1945. The penetration of irrigation and rain water into sandy soil of Central Florida. Soil Sci. Soc. Am. Proc. 10, 25–29.

Jury, W.A., Gardner, W.R., Gardner, W.H., 1991. Soil Physics, Wiley, New York (328pp).

King, P.M., 1981. Comparison of methods for measuring severity of water repellence of sandy soils and assessment of some factors that affect its measurements. Aust. J. Soil Res. 19, 275–285.

Kostka, S., 1997. Personal communications.

Letey, J., 1969. Measurement of contact angle, water drop

penetration time, and critical surface tension. In: Proc. Symp. Water Repellent Soils. Univ. Calif., Riverside, CA, pp. 43–47.

Liu, Y., Parlange, J.-Y., Steenhuis, T.S., Haverkamp, R., 1995. A soil–water hysteresis model for fingered flow data. Water Resour. Res 31, 2263–2266.

Marshall, T.J., Holmes, J.W., Rose, C.W., 1996. Soil Physics. 3rd ed., Cambridge University Press, Cambridge (453pp).

Miller, E.E., Miller, R.D., 1956. Physical theory for capillary flow phenomena. J. Appl. Phys. 27, 324–332.

Milly, P.C.D., 1988. Advances in modeling of water in the unsaturated zone. Transport Porous Media 3, 491–514.

Nieber, J.L., Bauters, T.W.J., Steenhuis, T.S., Parlange, J.-Y., 2000. Numerical simulation of experimental gravity-driven unstable flow in water repellent sand. J. Hydrology, 231–232, 295–307.

Nissen, H.H., Moldrup, P., de Jonge, L.W., Jacobsen, O.H., 1999. Time domain reflectometry coil probe measurement of water content during fingered flow. Soil Sci. Soc. Am. J. 63, 493–500.

Parlange, J.-Y., Hill, D.E., 1976. Theoretical analysis of wetting front instability in soils. Soil Sci. 122, 236–239.

Ritsema, C.J., Dekker, L.W., Nieber, J.L., Steenhuis, T.S., 1998. Modeling and field evidence of finger formation and finger recurrence in a water repellent sandy soil. Water Resour. Res. 34, 555–567.

Selker, J.S., Leclerq, P., Parlange, J.-Y., Steenhuis, T.S., 1992a. Fingered flow in two dimensions. 1. Measurement of matric potential. Water Resour. Res. 28, 2513–2521.

Selker, J.S., Steenhuis, T.S., Parlange, J.-Y., 1992b. Fingered flow in two dimensions. 2. Predicting finger moisture profile. Water Resour. Res. 28, 2523–2528.

Selker, J.S., Steenhuis, T.S., Parlange, J.-Y., 1996. An engineering approach to fingered vadose pollutant transport. Geoderma 70, 197–206.